Wall Modeling for Large-Eddy Simulation of Atmospheric Boundary Layers over Rough Terrain

Mohammad Abouali[1], **Bernard J. Geurts**[2,3], **Ambro Gieske**[1]

[1] International Institute for Geo-Information Science and Earth Observation
PO Box 6, 7500 AA Enschede, The Netherlands
[2] Multiscale Modeling and Simulation, Faculty EEMCS, University of Twente, PO Box 217
7500 AE Enschede, The Netherlands b.j.geurts@utwente.nl
[3] Anisotropic Turbulence, Fluid Dynamics Laboratory, Faculty of Applied Physics
Eindhoven University of Technology, PO Box 513, 5600 MB Eindhoven, The Netherlands

Abstract

Irrigation can boost agricultural crops in arid regions. To make optimal use of the available water resources, careful management is necessary. This relies ultimately on our understanding of water uptake by the crop, evaporation and turbulent transport in the atmospheric boundary layer over the fields. To build computational models that can offer quantitative support for this water/crop management-problem, the turbulent transport close to the Earth's surface needs to be properly represented. Ideally, this would involve no-slip conditions imposed at the multitude of structures, undulations and vegetation that is present at the surface. This is obviously unrealistic, from a computational perspective, but also since such detailed geometry information and complete knowledge of the interaction between flow and vegetation are not available. In this paper we review the much simpler approach of wall-modeling to describe turbulent flow over rough terrain. We illustrate its use for boundary layers developing over smooth walls and for uniformly rough walls. Then, we consider an extension toward spatially non-uniform roughness and investigate the development of the boundary layer over walls with stripe-patterns. The primary effects of wall-roughness appear to be well represented by simple wall modeling.

1 Introduction

Our daily lives are influenced most directly by physical, chemical and biological processes that take place in the first few hundred meters of the Earth's atmosphere. Transport in this so-called atmospheric boundary layer is dominated by turbulent flow [1, 2]. This affects the rate at which dispersion can take place. In urban regions this environmental dispersion connects to safety and health issues, because often the transport and dilution of pollutants is concerned [3]. In relation to crop management in arid regions, the dispersion of water vapor is of central importance. In either case understanding turbulent flow over rough terrain is of key importance.

The investigations in this paper are motivated by water management problems in agriculture. In many cases the available water is a precious commodity, and its use needs to be balanced with the economic pressures associated with crop production. The development of quantitative computational support for this complex problem is a timely challenge, also to fluid dynamicists. As the flow near the surface is a key building-block problem in this context, we will focus on the approximate modeling of turbulent flow over 'rough walls' to mimic effects of the local vegetation and landscape.

Figure 1: Irrigation equipment that pivots around central water supply points placed in an array creates an intriguing landscape (www.gearth.com).

The problematic relation between large-scale crop production and limited water supply is illustrated in Figure 1. The irrigation equipment takes its groundwater from a central point around which it pivots. This creates circles in which crop can develop, and sharp boundaries with the natural, arid surrounding. The vapor transport in the atmospheric boundary layer over this landscape is crucial for the optimal water supply 'protocol'. Decisions need to be made about when to supply the next batch of water, how much, over what length of time, etc., etc.

Today's spatially well resolved satellite imagery opens new possibilities for water management. The continuous flow of information about local and regional meteorological conditions and a precise specification of the local topography and (time-dependent) surface-conditions, can be integrated into a computational fluid dynamics model. This creates the possibility to develop a model-system to predict the effect of different irrigation protocols under a variety of environmental and atmospheric conditions.

Resolving all details of a turbulent flow as it develops over a specific landscape, provides conceptually the simplest fluid dynamics model for the flow near the Earth's surface. A mathematical model would in that case be based at least on the Navier-Stokes equations, the no-slip boundary condition applied at all solid objects, and flow-structure interaction, incorporating flow over crop fields, through canopies, over and around even the smallest branches and twigs. It is immediately clear that this is a naive suggestion. The amount of detail that would

be required can not be dealt with from a computational point of view, but is also not available to us.

Most water management issues only require knowledge of the primary turbulent transport processes. Hence, it appears that some level of modeling of the turbulent flow and its modulation by the underlying 'rough' surface can be introduced, guided by our knowledge of the flow-physics. A helpful first distinction can be made between the flow nearest the surface and the turbulence in the outer 'bulk' flow [4]. The complexity of the description of the flow-dynamics in each of these regions can be reduced in specific ways. Turbulence in the outer shear flow can be addressed in considerable detail using large-eddy simulation. The flow nearest the surface will be addressed by introducing approximate wall modeling [5]. These approximations will be discussed briefly next.

Capturing turbulent flow in all its detail in the 'outer' layer, i.e., well enough separated from the Earth's surface, is hard when use is made of so-called direct numerical simulation. In this case, all length- and time-scales of the turbulent flow should be resolved numerically. For realistic atmospheric flow conditions, this requires an amount of computational detail that can not be processed with currently available computers [6]. A modeling approach that is based on a statistical description of turbulence is available in the form of Reynolds averaged Navier-Stokes (RaNS). For predictions of general features, the RaNS approach may offer some understanding of the flow-physics. However, in case time-dependent and spatially localized information is required, the RaNS approach may not be acceptable as it often adopts turbulence models that contribute too much dissipation of small features. In addition, the accuracy with which boundary layer flow is predicted is somewhat limited. To obtain a computational modeling that is both feasible, i.e., not DNS, and allows capturing of time-dependent turbulence at considerable but controllable spatial resolution, the contours of an alternative method exist in the form of large-eddy simulation.

In large-eddy simulation one allows smoothing of a turbulent flow by low-pass spatial filtering [8]. Hence, an external control over the size of the smallest resolved length-scales becomes available. In fact, flow structures that are smaller than the 'width' of the filter are effectively removed from the flow-description, which significantly reduces the complexity of the computations. Filtering the nonlinear convective terms in the momentum equations introduces a closure problem [8, 9]. This closure problem is expressed in terms of the turbulent stress tensor and is directly related to the dynamical consequences of the flow-structures that were removed by the spatial filter. An extensive literature documents approximate modeling of the turbulent stresses in terms of so-called sub-grid or sub-filter models. These require knowledge of the filtered flow only and yield computational models that capture the primary aspects of canonical boundary layer flows quite well. Examples of sub-filter models include regularization models [10, 11] and dynamic models, based on the Germano-Lilly procedure [12].

One of the current pacing items in the development of large-eddy simulation is the effective treatment of flow in the vicinity of solid surfaces. This is also the region from where important contributions to the vapor transport in the atmospheric boundary layer originate. Since complete numerical resolution of the near wall region is not a viable option with current computational resources, a more efficient, albeit approximate treatment of this region is required. Various ingenious proposals have been made, ranging from extensive zonal approaches to much simpler equilibrium models [6, 7]. We will concentrate on the latter class of models and follow the pioneering work by Schumann [5]. In Section 2 we discuss the famous law-of-the-wall, which motivates the wall modeling considered here. In Section 3 we discuss the application of this method to boundary layers over flat walls with uniform roughness. Section 4 describes effects of spatial non-uniformities in the surface roughness and concluding remarks are collected in Section 5.

2 Law-of-the-wall

In this section we first review the law-of-the-wall and then sketch its use to obtain approximate boundary conditions for the 'outer' turbulent flow. The roughness length-scales are assumed to be considerably smaller than the thickness of the atmospheric boundary layer. Under this condition, the effects of surface-roughness is traditionally captured in a single roughness parameter [13].

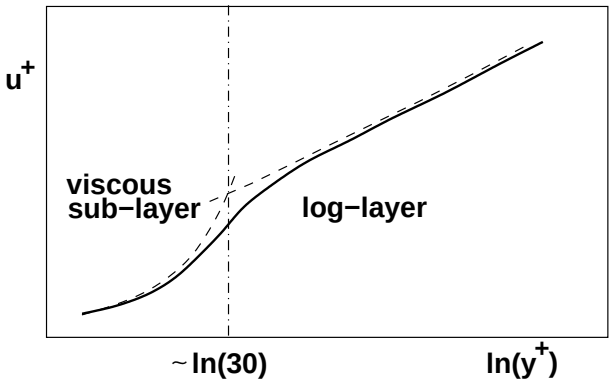

Figure 2: Near-wall boundary layer structure expressed in wall-coordinates. The solid line represents the average streamwise velocity, which is approximated by $u^+ = y^+$ in the viscous sub-layer and shows $u^+ \sim \ln(y^+)$ in the logarithmic layer.

The structure of a turbulent boundary layer over a smooth flat surface has been the subject of many studies. Over the years multi-layered descriptions have emerged. The simplest one, used in this paper, is summarized in Figure 2. Nearest the wall the average flow in the streamwise direction is given in so-called wall-coordinates by:

$$\begin{aligned} u^+ &= y^+ \quad ; \quad 30 \gtrsim y^+ \geq 0 \\ &= \frac{1}{\kappa}\ln(y^+) + b^+ \quad ; \quad y^+ \gtrsim 30 \end{aligned} \tag{1}$$

Here $u^+ = \langle u \rangle / u_\tau$ and $y^+ = (y u_\tau)/\nu$ in terms of the wall-normal coordinate y, the average streamwise velocity $\langle u \rangle$, the kinematic viscosity ν and the friction velocity u_τ. The latter is defined as $u_\tau = (\tau_w/\rho)^{1/2}$ with fluid density ρ and wall shear-stress $\tau_w/\rho = \nu d\langle u \rangle/dy$ evaluated at $y = 0$. The averaging operator $\langle \cdot \rangle$ may be interpreted as average over time for statistically stationary flows. In (1) the Von Kármán constant $\kappa \approx 0.4$ and the off-set is given by $b^+ \approx 5.2$ [14]. In meteorological literature b^+ is often absorbed into a length-scale parameter y_0^+ defined through $b^+ = -\ln(y_0^+)/\kappa$ and we may write

$$u^+ = \frac{1}{\kappa}\ln\left(\frac{y^+}{y_0^+}\right) \tag{2}$$

The above values for κ and b^+ yield $y_0^+ \approx 0.125$ for turbulent flow over a smooth wall.

The parameter y_0^+ is often re-interpreted as a roughness length-scale [13]. For walls that have an irregular rough surface the roughness parameter $y_0^+ \equiv (Du_\tau)/\nu$ where D denotes the average amplitude of surface undulations of the wall. By allowing y_0^+ to be a function of the in-wall coordinates x and z, one may incorporate spatial variations in local roughness and thereby arrive at a formulation for approximating different local conditions on the Earth's surface. Connected to detailed satellite imagery, this identification allows to phenomenologically characterize particular regions in terms of their 'roughness map'. In this paper we will assume D to be independent of time and externally specified. An increase in the roughness parameter directly affects the convective transport near the Earth's surface. Near-surface transport of scalars, such as vapor over a crop field, is frequently described in a similar fashion but requires the introduction of a second roughness map z_0^+ [15].

So far, the law of the wall was used only for interpretation purposes. However, as pioneered by Schmidt and Schumann [5], the assumption of the logarithmic dependence of u^+ on y^+ can also be used to define alternative boundary conditions for the 'outer' turbulent flow. This will be referred to as wall-modeling. Instead of imposing no-slip conditions at the wall $y = 0$, one may extract a logarithmic extrapolation procedure for the streamwise velocity at some height $y = y_b$ inside the log-layer [16]. This proceeds in a few steps. Assume 'average' velocities $\langle u_1 \rangle$ and $\langle u_2 \rangle$ to be given at (x, y_1, z) and (x, y_2, z). Throughout we work with $y_b^+ \approx 70$ and $y_{1,2}^+$ in the range up to 100. Assuming the logarithmic velocity profile to be valid at each of the y-locations, one may reconstruct the friction velocity as

$$u_\tau = \frac{\kappa(\langle u_2 \rangle - \langle u_1 \rangle)}{\ln(y_2/y_1)} \tag{3}$$

With u_τ known, one may extract u_b^+ at y_b^+ by evaluating the logarithmic law and subsequently obtain the actual u_b at $y = y_b$. Various implementations of this basic procedure have been formulated in literature [5, 17, 18, 6]. It is beyond the scope of this paper to discuss these in any details. Differences are often quite subtle and not easy to appreciate. By invoking this procedure, one may 'skip' the explicit computation of the flow nearest the wall and still maintain compliance with the assumed logarithmic profile.

The implementations of the effective 'law-of-the-wall boundary condition' at the edge of the 'outer' turbulent flow distinguish a variety of averaging operators $\langle \cdot \rangle$. So far, we interpreted $\langle \cdot \rangle$ as time-average. Often, averaging over the in-wall coordinates x and z is included as well. This may well be motivated in case of flow over uniformly roughed walls, but it appears not the optimal choice in case some of the details of the roughness-map need to be taken into account. Alternative averages could involve averaging over time and only the z-coordinate, or only the x-coordinate, or no averaging at all but simply invoking the log-law for the local instantaneous solution. In the next section we consider flow over walls with uniform roughness and compare results obtained from different averaging procedures.

3 Uniformly roughed walls

We consider flow over a flat plate with uniform roughness. The simulation set-up is sketched in Figure 3. We adopt a Reynolds number $Re = 10^4$ based on the boundary layer thickness, and a computational box with $y_u = 10$ and extent in the streamwise and spanwise direction of 4π and $4\pi/3$ respectively. In case wall-modeling is applied, the edge of the computational domain is located at $y_b \approx 2$, which is well inside the log-layer for the cases considered. The computational grid uses $n_x \times n_y \times n_z$ grid cells – we typically employ $n_{xyz} = 32$ or 64, with a uniform grid in the streamwise and spanwise directions and a grid that is clustered near the wall in the y-direction. The flow is forced by a time-dependent mean pressure gradient that maintains a constant mass-flow [19]. No explicit sub-filter model was introduced at this stage. The coarse-grid simulations were found to be of acceptable accuracy on their own, at the selected flow-conditions. This provides a good testing-ground for the development of the wall-modeling. The numerical method is based on explicit time-stepping and a fourth order accurate skew-symmetric finite volume discretization of the convective fluxes and a positive definite discretization of the viscous fluxes [19, 20].

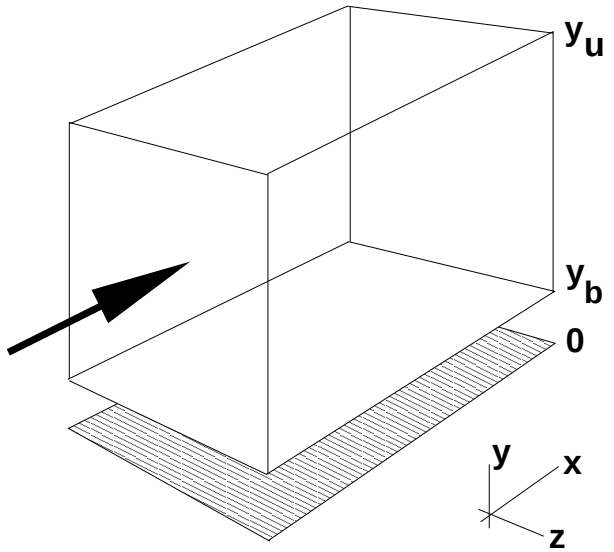

Figure 3: Computational domain used for turbulent boundary layer simulations over a uniformly roughed wall. The actual wall is shown hatched. The lower edge of the computational box for the 'outer' flow is located at $y = y_b$. Periodic conditions apply in the x and z directions and a free-slip condition is used at $y = y_u$.

In order to validate the wall model and assess the sensitivity of the results on the averaging operator, the mean streamwise velocity is plotted in Figure 4 for flow over a smooth wall. First, we observe that, even at the coarse resolution used, the results obtained with the no-slip wall condition correspond quite closely to high-resolution DNS data [21]. The results obtained with the wall model and different averaging operators all show a slight shift toward higher values of y^+. However, the qualitative features of the boundary layer flow are well captured. The differences due to different averaging operators are modest. When comparing the mean streamwise velocity profile plotted as a function of the physical coordinate y, the differences are much less visible, showing that the differences arise mainly from a slight

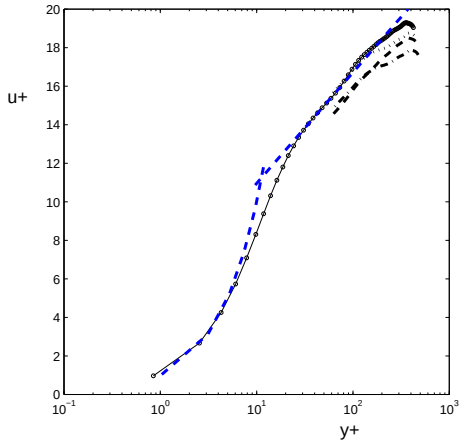

Figure 4: Mean streamwise velocity for flow over a smooth wall. We compare data from DNS (solid) with coarse grid simulations ($n_x = n_z = 32$, $n_y = 64$) that use no-slip conditions at the wall ($\circ$), or a wall model applied at $y_b^+ \approx 65$ and based on (t, x, z) averaging (dashed), (t, z) averaging (dotted) and t averaging (dash-dotted). The viscous sub-layer and the log-layer are clearly observable.

over-estimation of the friction velocity u_τ.

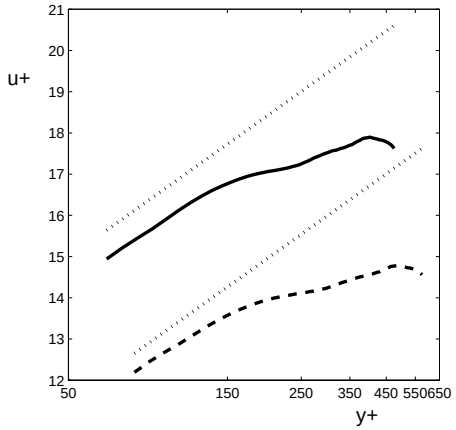

Figure 5: Mean streamwise velocity for flow over a smooth wall (solid) and a uniformly roughed wall at $y_0^+ = 0.5$ (dashed) compared to the log-law results (dotted). Wall modeling was applied at $y_b^+ \approx 65$ in combination with time-averaging.

We now turn to the effect of wall roughness. We adopt $y_0^+ = 0.5$, which is four times larger than used above. The mean streamwise velocity is shown in Figure 5, where use was made of the time-averaging operator. We notice directly the strong reduction in u^+ at the same y^+ coordinate. This trend corresponds qualitatively with the expected effect of a rough wall condition. The simple wall-model hence allows to properly capture the primary response of the boundary layer to variations in the roughness parameter. Since the differences due to the specific averaging operators were found to be only small, we will adopt the time-averaging method in the sequel. Some results obtained for simple roughness variations will be discussed in the next section.

4 Non-uniform roughness patterns

In this section we present some preliminary results illustrating the effect of variations in the local roughness. The final goal is to predict boundary layer flow over very complex roughness-maps that correspond to actual landscapes, cf. Figure 1. Here, we consider the basic problem of the response of the boundary layer to strips of rough surface, placed in the spanwise direction, i.e., normal to the mean flow.

We consider two roughness patterns. In pattern A we consider one strip of rough wall with $y_0^+ = 0.5$ in an otherwise smooth wall. The width of the rough strip equals one quarter of the streamwise domain-length. This case is selected to investigate the rate at which a perturbed rough-surface boundary layer recovers toward the smooth wall situation. In pattern B we consider the sequence smooth-rough-smooth-rough, with strips of equal width.

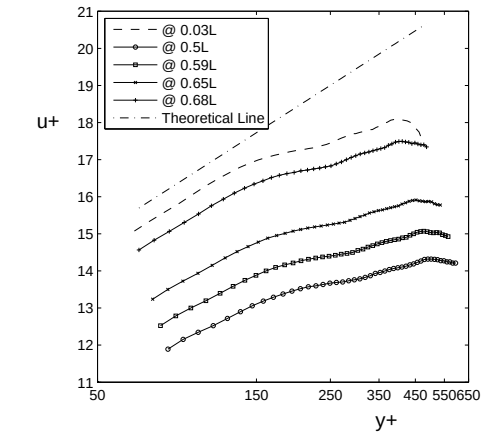

(a)

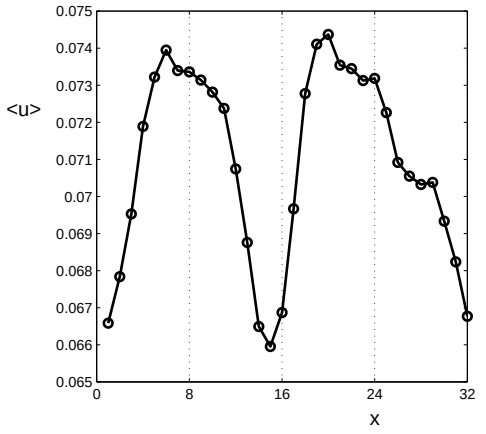

(b)

Figure 6: Mean streamwise velocity for flow over a wall with non-uniform roughness pattern. The rough patches are characterized by $y_0^+ = 0.5$, and are included in an otherwise smooth wall. In (a) we consider a strip of width $L/4$ around $x = L/2$ across the spanwise domain, quantifying the deviation from the smooth wall. The label refers to the x-location at which the profile is monitored, in units of the streamwise domain length. In (b) two rough patches of width $L/4$ are interlaced with two smooth patches of width $L/4$. This displays the deviation from and restoring of the smooth-wall boundary flow. The non-periodicity of the pattern is an indication of the time-averaging accuracy.

In Figure 6(a) we collected the effect of pattern A

roughness in terms of the velocity field in wall coordinates. Entering the rough patch in the downstream direction, we notice that the shape of the streamwise velocity profile remains quite similar to that of the smooth wall condition. However, inside the rough patch the basic 'smooth-wall' profile is shifted considerably toward lower velocities. This trend was also observed when comparing a uniformly roughed wall with a smooth wall in the previous section. As the end of the rough patch is approached, a gradual recovery of the smooth-wall velocity profile is observed.

In Figure 6(b) the results obtained for the periodic roughness pattern B are shown. We plot the variation in the mean streamwise velocity as a function of the downstream direction. Results are shown for the u-velocity near the bottom boundary where the wall-modeling is applied. The plot contains the u velocity, additionally post-processed by averaging over t and z. The vertical, dotted lines correspond to the boundaries between the rough and smooth patches. Upon entering a rough patch, the reduction in the velocity is first quite gradual, and then rather abruptly. The recovery to the smooth wall profile shows the reverse trend – the flow returns rather quickly to the smooth wall profile. These applications of the wall-model confirm that this simple treatment does appear to capture the main features of flow over rough surfaces.

5 Concluding remarks

We briefly sketched the problem of water/crop management in arid regions and its relation to turbulent transport in atmospheric boundary layers. In order to arrive at manageable computations, an element of physical modeling of the flow over rough surfaces was put forward. In this model we assume that the characteristic log-layer applies to the rough-wall flow. This gives us the opportunity to formulate alternative boundary conditions inside the log-layer and effectively avoid the need to resolve the high-gradient region closest to the wall.

Different averaging operators were compared. It was found that the long-time averaging yields accurate results, compared to high-resolution DNS, employing no-slip wall conditions. A validation for flow over uniformly roughed walls confirmed the general level of accuracy. This method was then adopted to rough walls with a non-uniform roughness pattern in the form of stripes perpendicular to the main flow. The primary effects of wall roughness on the boundary layer flow were recovered successfully. A more quantitative comparison and parameter-study is underway and will be published elsewhere.

The computational effort can be reduced considerably when use is made of the log-layer wall modeling. First of all, the number of grid-points can be significantly reduced. Second, the smallest grid-cells in the wall-normal direction can be made much larger compared to the no-slip wall application. This implies that a considerably larger time-step can be used in the simulation.

In order to arrive at computational support for the agricultural applications mentioned, the computations should be integrated with external data-streams arising from real-time satellite-imagery and/or field measurements. This is a challenging topic of future research.

Bibliography

[1] Stull, R.B., 1999. An Introduction to Boundary Layer Meteorology, 1. Springer, 684 pp.

[2] Oke, T.R., 1988. Boundary Layer Climates, 1. Routledge, 450 pp.

[3] Holtslag, A.A.M. and Ek, M., 1996. Simulation of surface fluxes and boundary layer development over the pine forest in Hapex-Mobilihy. Journal of Applied Meteorology, 35:202-213.

[4] Pope, S.B., 2000. Turbulent Flows, 1. Cambridge University Press, 770 pp.

[5] Schmidt, H. and Schumann, U., 1989. Coherent structures of the convective boundary layer derived from large-eddy simulation. J. Fluid Mech., 200: 511-562.

[6] Piomelli, U. and Balaras, E., 2002. Wall-layer models for large-eddy simulations. Annual Review of Fluid Mechanics, 34: 349-374.

[7] Piomelli, U., Balaras, E., Pasinato, H., Squires, K.D. and Spalart, P.R., 2003. The inner-outer layer interface in large-eddy simulations with wall-layer models. Int. J. Heat Fluid Flow, 24:538-550.

[8] Geurts, B.J., 2004. Elements of Direct and Large-eddy Simulation, 1. Edwards, 344 pp.

[9] Sagaut, P. and Meneveau, C., 2004. Large Eddy Simulation for Incompressible Flows 1.Springer, 426 pp.

[10] Geurts, B.J., Holm, D.D.: 2003. Regularization modeling for large-eddy simulation. *Phys. of Fluids*, **15**, L13

[11] Geurts, B.J., Holm, D.D.: 2006. Leray and NS-α modeling of turbulent mixing, *J. of Turbulence*, **7** (10), 1 - 33.

[12] Germano, M., Piomelli U., Moin P., Cabot W.H.: 1991. A dynamic subgrid-scale eddy viscosity model. *Phys.of Fluids*, **3**, 1760.

[13] Raupach, M.R., Antonia, R.A. and Rajagopalan, S., 1991. Rough-Wall Turbulent Boundary Layers. Applied Mechanics Reviews, 44(1): 1 - 26.

[14] Zanoun, E.S., Durst, F. and Nagib, H., 2003. Evaluating the law of the wall in two dimensional fully developed turbulent channel flows. Physics of Fluids, 15(10): 3079-3089.

[15] Brutsaert, W., 1982. Evaporation into the Atmosphere 1. Springer, 316 pp.

[16] Albertson, J.D., 1996. Large eddy simulation of land-atmosphere interaction, Thesis University of California, 185 pp.

[17] Moeng, C.H., 1984 A large eddy simulation for the study of planetary boundary layer turbulence, J. Atmos. Sci., 41, 2052-2062.

[18] Mason, P.J., 1989, Large-eddy simulation of the convective atmospheric boundary layer, J. Atmos. Sci., 46, 1492-1516.

[19] Verstappen, R. and Veldman, A.E.P., 2003. Symmetry-preserving discretization of turbulent flow. Journal of Computational Physics, 187(1): 343-368.

[20] Verstappen, R. and Van der Velde, R.M., 2006. Symmetry-preserving discretization of heat transfer in a complex turbulent flow. Journal of Engineering Mathematics, 54(4): 299-318.

[21] Verstappen, R. and Veldman, A.E.P., 1997. Direct numerical simulation of turbulence at lower costs. Journal of Engineering Mathematics, 32(2-3): 143-159.